Age spot or youthful marking: The origin of Reiner Gamma

Joseph B. Nicholas

Washington International School, Washington D.C., USA

Michael E. Purucker

Raytheon at Planetary Geodynamics Laboratory, NASA/GSFC, Greenbelt, Maryland, USA

Terence J. Sabaka

Raytheon at Planetary Geodynamics Laboratory, NASA/GSFC, Greenbelt, Maryland, USA

Abstract. The highly magnetic (field magnitudes of 50 nT at 18 km altitude) Reiner Gamma albedo feature on the near side of the moon has been explained in terms of differential space weathering of an old feature, or a recent cometary impact. We investigated this feature using magnetometer data from Lunar Prospector. The magnetic sources lie within a few km of the surface, and are magnetized in a north-south direction. The strength of the magnetization is spatially related to the albedo of the feature, and the minimum magnetization necessary to explain the magnetic field observations varies from 100 A/m for a 10 m thick layer, to 1 A/m for a 1 km thick layer. These constraints point towards an origin of the magnetic field signal as due to basin impact ejecta, and the origin of the albedo feature as a consequence of retarded ageing under the umbrella of the Reiner Gamma mini-magnetosphere.

0094-8276/06/$5.00

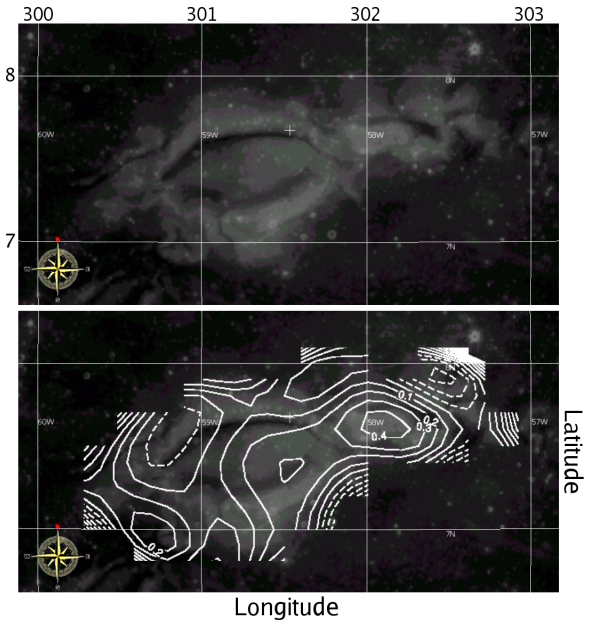

Figure 1. Gray-scale image showing the main part of the Reiner Gamma formation (high albedo region). This Clementine image was acquired by the UV-VIS camera and represents a single spectral band (30XX). The overlay shows the magnitude of the magnetization in a northerly direction over Reiner Gamma (solid lines are positive, dashed lines are negative). The contour lines are at 0.1 A/m intervals, and assume an arbitary 40 km thick crust.

1. Introduction

Reiner Gamma is an enigmatic feature, visible from the Earth with a small telescope (see figure 1), that is associated with one of the strongest magnetic anomalies on the Moon. It is located at approximately 7.5°N 59.0°W. One of a class of objects termed 'swirls', its age is controversial and its relation to the magnetic anomaly unknown. Swirls are albedo markings that characteristically exhibit winding or sinuous patterns. Reiner Gamma is thought to be of either Eratosthenian or Copernican age [*Wilhelms*, 1987]. There are two models for the origin of the albedo markings, as the relict of a recent (< 1 Myr old) cometary impact [*Starukhina and Shkuratov*, 2004] or related to the deflection of the solar wind [*Richmond et al.*, 2005]. Its alignment approximately radial to the center of the Imbrium basin [*Hood et al.*, 2001] suggests that Imbrium basin ejecta units may be the source.

We apply techniques developed to study terrestrial magnetic anomalies to assess the depth to the source of this magnetic feature, the spatial distribution of the magnetization, and it's magnitude.

2. Data

The vector fluxgate magnetometer onboard Lunar Prospector (1998-1999) was utilized for this study. Level 1B data were acquired from the NASA Planetary Data System node at the University of California, Los Angeles. The data were converted to a local horizontal coordinate system with B_r positive outward, B_θ positive southward, and B_ϕ positive eastward. As in the study of *Kurata et al.* [2005], the data were selected from the six quietest days, 5 in the lunar wake, and 1 in the earth's geomagnetic tail lobe.

The data used over the Reiner Gamma region were taken at altitudes between 18 km and 40 km (see figure 4). Depth to source calculations are more accurate when data are available at multiple altitudes, and those altitudes are comparable to the thickness of the magnetic layer. The electron reflectometer data [*Halekas et al.*, 2001] confirm the location and strength of the Reiner Gamma anomaly, but are not utilized in the present study.

3. Model

3.1. External Magnetic Field

Prior to the analysis, a simple model of the external magnetic field was removed from the Lunar Prospector data.

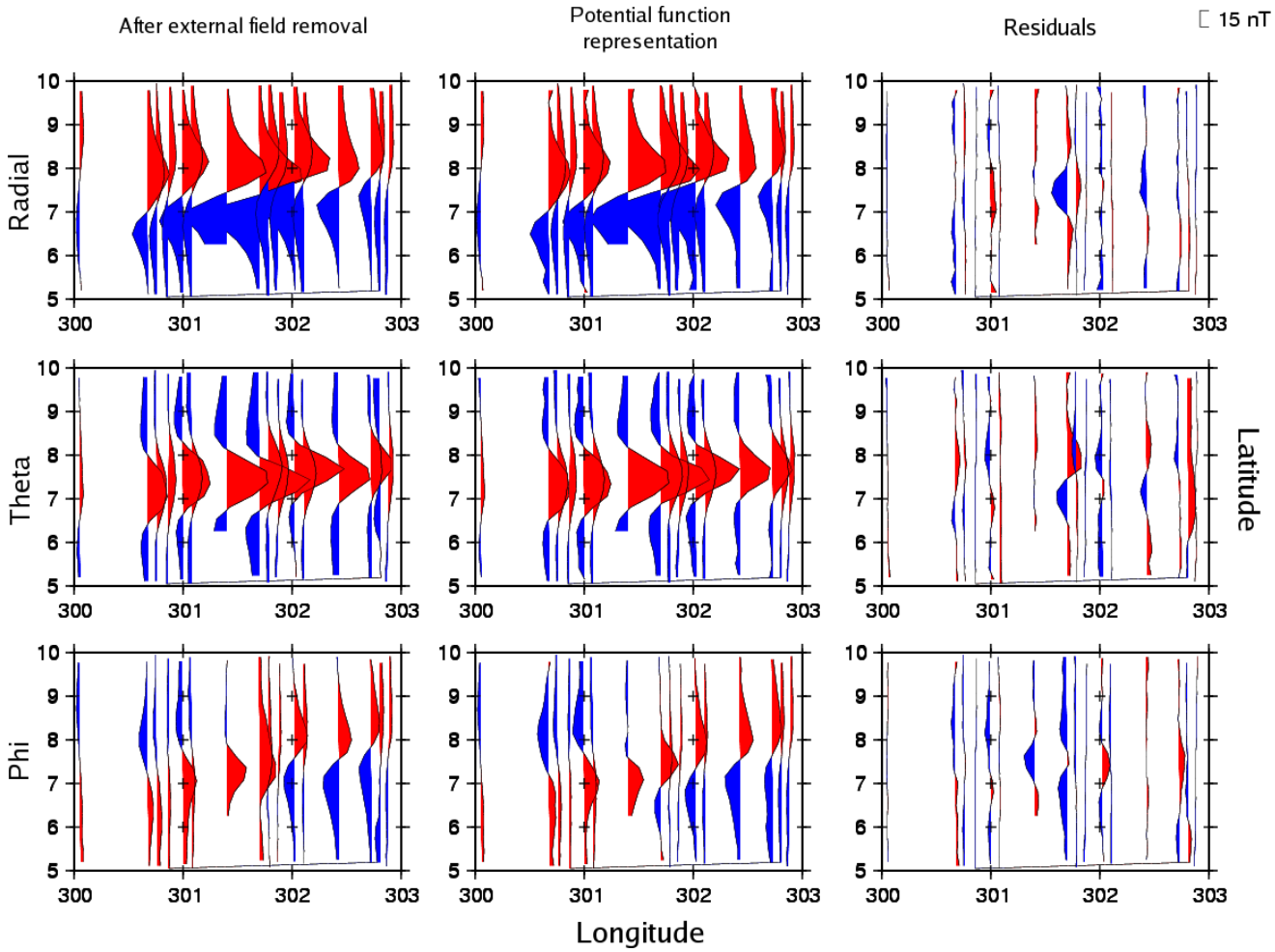

Figure 2. Stacked profile plots showing the actual magnetic field data after external field removal (left), the modeled internal component (center), and the remaining unfit field (right) above Reiner Gamma. The three components shown are B_r (top), B_θ (center), and B_ϕ (bottom). Red colors indicate positive fields, blue are negative. The scale bar in the upper right indicates the magnitude of the field. The RMS values for the B_r, B_θ and B_ϕ residuals are 1.99, 2.43 and 1.65 nT, respectively. Note that the magnetic field is horizontal over the center of Reiner Gamma, and bounded to the north and south by steeply dipping magnetic fields. This feature is most simply interpreted in terms of a body with a horizontal, N-S oriented magnetization approximately coincident with the Reiner Gamma feature. As a consequence, the internal field was modeled as a grid of horizontal, N-S directed dipoles.

The external field was parameterized as a uniform field over each satellite half-orbit, extending from north pole to south pole. The external field was determined from all three components of the vector data in a least-squares sense. This approach has previously been shown [*Purucker et al.*, 2006] to yield directions that are in good agreement with the standard T96 model of the earth's magnetosphere [*Tsyganenko*, 1996], at times when the moon is in the earth's magnetic tail. It differs from the component by component, along-track filter approach of *Hood et al.* [2001] in treating the external field as a potential field.

The E-W separation of adjacent passes (Figure 2) is less than or equal to the altitude above the surface, meaning that fields of internal origin will appear on multiple passes. In the course of one earth day, Lunar Prospector will cover a swath approximately 12 degrees wide in E-W dimension, and successive orbits advance approximately 1 degree in longitude.

3.2. Minimum magnetization

Ideal body analysis [*Parker*, 2003] systematizes the process of placing bounds on the distribution of magnetization via the minimization of the infinity norm of the magnetic intensity within the source region. Figure 5 shows the minimum magnetization required for a given layer thickness, irrespective of the magnetization direction. The equation used to calculate this curve is as follows [*Parker*, 2003]:

$$M \geq M_0 = \frac{12|\mathbf{B}|/\mu_0}{[6+\sqrt{3}\ln(2+\sqrt{3})]\ln(h_2/h_1)}.$$

M_0 is the minimum magnetization, $|\mathbf{B}|$ is the magnitude of the maximum observation, h_1 is the altitude, and h_2 is the altitude plus layer thickness such that $h_2 - h_1$ equals the layer thickness. This figure was generated using a value of $|\mathbf{B}|$ of 49.0783 nT at an altitude of 18.520 km.

3.3. RMS minimization

The vector magnetic field observations were fit in a least-squares sense to a grid of magnetic dipoles [*Dyment and Arkani-Hamed*, 1998; *Purucker et al.*, 1996] extending over the entire region shown in Figure 2. A spherical coordinate system was used throughout the analysis. Note that

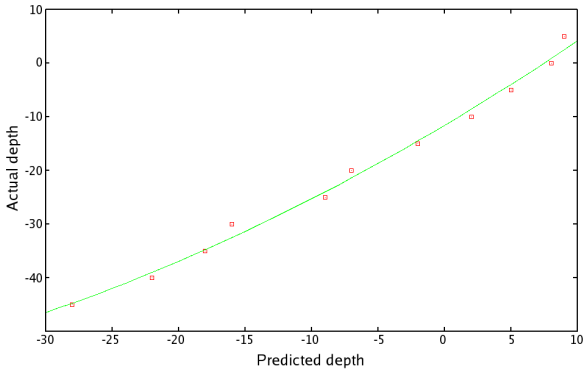

Figure 3. Calibration curve used to adjust the results. The equation of the fit is $d_a = 0.010d_p^2 + 1.473d_p - 11.56$. Negative values are below the surface, positive values are above.

the magnetic field is horizontal over the center of Reiner Gamma, and bounded to the north and south by steeply dipping magnetic fields. This feature is most simply interpreted in terms of a body with a horizontal, N-S oriented magnetization approximately coincident with the Reiner Gamma feature. As a consequence, the internal field was modeled as a grid of horizontal, N-S directed dipoles. The individual dipoles were separated by a quarter of a degree. In order to calculate the depth of the magnetic source, the predicted field was calculated with the source grid at depths from 15 km above the surface to 40 km below the surface, in one km increments. The difference between this predicted field and the observed data (after removal of the external field), was then calculated, and the RMS of these differences calculated. The depth of the magnetic source is then obtained by finding the minimum in a plot of RMS misfit vs depth below the surface.

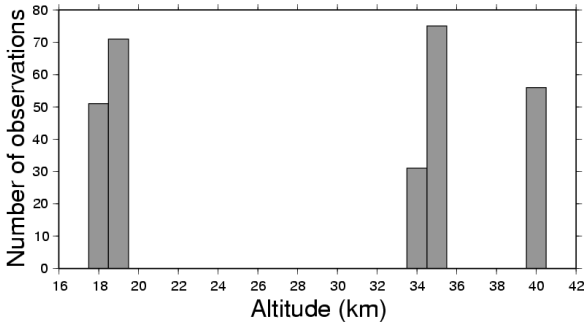

Figure 4. The distribution of altitudes in the data used over the main part of Reiner Gamma.

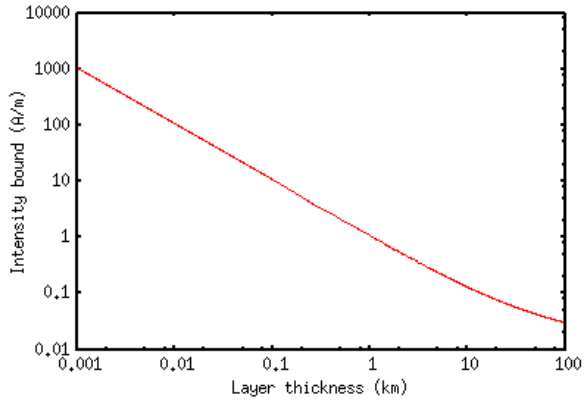

Figure 5. Minimum source magnetization required to explain a field magnitude of 49.078 nT at an altitude of 18.520 km.

3.4. Calibration

After conducting some model studies, it became obvious that there was a small but consistent offset between the actual depth of the dipoles and the depth that the model was predicting. To account for this offset, a calibration curve was developed. First, the magnetic field from a dipole at known depth was calculated at altitudes between 20 and 40 kilometers. The predicted depth of that source was then calculated using the RMS minimization technique described above. After repeating this process for known depths between 0 and 40 kilometers, a plot was made of actual depth vs predicted depth, and a quadratic was fit to these points (see figure 3). This function could then be used to adjust the predicted depths when using the model.

As different dipole spacings, locations, and magnetization directions yielded different calibration curves, the parameters for the model were chosen to be the same as that of Reiner Gamma when making the calibration curve.

3.5. Calibrated depth to source

Based on a grid of quarter degree northward facing dipoles, the depth of the main part (SW) of the Reiner Gamma formation is approximately 7 kilometers above the surface based on the radial component, 8 km above the surface based on the north/south component, and 13 km below the surface based on the east/west component (see figure 6). Converting these values to an actual depth based on the calibration curve in figure 3 yields a depth of approximately 1 km below the surface for the radial component, 1 km above the surface for the north/south component, and 29 km below the surface for the east/west component.

These results suggest that the magnetic sources under Reiner Gamma are near the surface. As can be seen from Figure 2, while the radial and theta components have high signal/noise ratios, the phi component does not. External fields associated with magnetic boundary effects are often

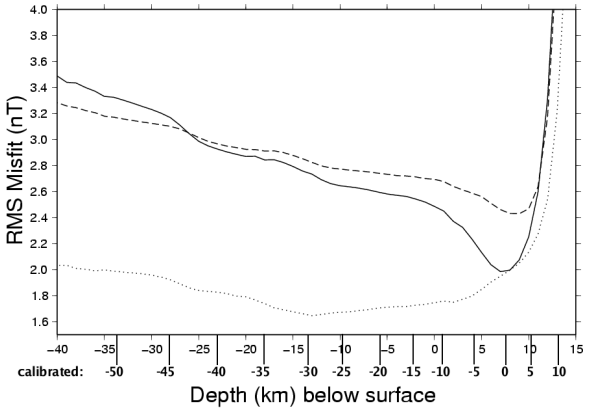

Figure 6. The minimum on each component represents the calculated depth. The solid line is based on B_r, the dashed on B_θ and the dotted on B_ϕ. Positive values are above the surface. On the x-axis, the top numbers represent the predicted depth, and the bottom numbers represent the depth after calibration.

encountered in the horizontal components, especially the phi component, in the lunar or Martian environments. We have not attempted to model these fields in this study, and hence we expect larger uncertainties in the horizontal components.

3.6. Spatial distribution of magnetization

In order to assess the spatial distribution of magnetization, we placed a grid of dipoles under only the albedo pattern. As before, the dipole directions were forced to lie in the north-south direction. The dipoles were separated by 0.1 degrees. We then solved for the magnitude and sign of these dipoles, and the results are shown in Figure 1. The magnetizations are seen to be most intense in the 'neck' of the feature, where albedos are highest, and decrease with decreasing albedo in both WSE and E directions.

4. Discussion

The shallow source of the Reiner Gamma feature is consistent with previous studies using different approaches. *Kurata et al.* [2005] found a source at 11.1 km using a single dipole whose parameters were determined in an iterative approach. The shallow source suggests that the origin is most simply explained as a near-surface ejecta layer, perhaps from Imbrium [*Hood et al.*, 2001], or as a cometary impact. An ejecta layer would require magnetizations of 1 A/m if it were 1 km in thickness, or 10 A/m if it were 100 m in thickness. The dominant magnetic remanence carriers on the moon are native iron-bearing alloys, and such magnetization strengths have been reported in previous studies [*Fuller*, 1998].

The Reiner Gamma region is one of the most magnetic on the moon, and has been shown to exhibit features characteristic of a mini-magnetosphere above it [*Kurata et al.*, 2005] which can stand off the solar field during quiet and slightly disturbed conditions. The spatial relationship of the inferred magnetization strength (Figure 1) with albedo is suggestive of an origin related to ageing in the solar wind. The minimum magnetization required to explain the feature argues most strongly for an ageing origin, with the source in the material underlying the surface albedo feature. Magnetizations in excess of 100 A/m would be necessary to explain a 10 m thick layer of cometary ejecta at or near the surface. More realistic thickness of cometary debris, say 1 m in thicknes, would require magnetizations in excess of 1000 A/m. Such magnetizations have never been encountered in nature over such a wide area, and even high concentrations of metallic iron, or iron-nickel alloys, in the cometary debris, seem inadequate to explain such a large scale and coherent magnetic signal.

Uncertainties in this investigation that could potentially have affected the results include the location and spacing of the dipoles, and the magnetization of the body. In order to compensate for these uncertainties, we have developed a calibration curve that was made using parameters as close as possible to those used for Reiner Gamma (i.e. same dipole spacing, location, and similar field magnitude).

The magnetization direction of Reiner Gamma is unknown, although the field directions over the body strongly suggest that the magnetization is horizontal, and in the N-S direction.

5. Conclusion

The results from this study suggest that the magnetic source of Reiner Gamma is most likely very close to the surface, between the surface and 1 kilometer deep. An origin as an ejecta layer from the Imbrium impact is strongly preferred, especially in light of the very high magnetizations that would be required for thin sheets of cometary ejecta. The spatial correspondence of the magnetization strength with albedo also argues for an ageing origin, where the strength of the magnetic field in Reiner Gamma stands off the solar wind under quiet and slightly disturbed conditions.

References

Dyment, J., and J. Arkani-Hamed (1998), Equivalent source dipoles revisited, *Geophys. Res. Lett.*, *25*, 2003–2006.

Fuller, M. (1998), Lunar magnetism – a retrospective view of the apollo sample magnetic studies, *Phys. Chem. Earth*, *23*, 725–735.

Halekas, J. S., D. L. Mitchell, R. P. Lin, S. Frey, M. H. Acuña, and A. B. Binder (2001), Mapping of lunar crustal magnetic fields using lunar prospector electron reflectometer data, *J. Geophys. Res.*, *106*, 27,841–27,852.

Hood, L. L., A. Zakharian, J. Halekas, D. L. Mitchell, R. P. Lin, M. H. Acuña, and A. B. Binder (2001), Initial mapping and interpretation of lunar crustal magnetic anomalies using Lunar Prospector magnetometer data, *J. Geophys. Res.*, *106*, 27,825–27,839.

Kurata, M., H. Tsunakawa, Y. Saito, H. Shibuya, M. Matsushima, and H. Shimizu (2005), Mini-magnetosphere over the Reiner Gamma magnetic anomaly region on the Moon, *Geophys. Res. Lett.*, *32*, L24205, doi:10.1029/2005GL024097.

Parker, R. L. (2003), Ideal bodies for Mars magnetics, *J. Geophys. Res.*, *108*, 5006, doi:10.1029/2001JE001760.

Purucker, M., T. Sabaka, and R. Langel (1996), Conjugate gradient analysis: a new tool for studying satellite magnetic data sets, *Geophys. Res. Lett.*, *23*, 507–510.

Purucker, M., T. Sabaka, N. Tsyganenko, N. Olsen, J. Halekas, and M. Acuña (2006), The Lunar magnetic field environment: interpretation of new maps of the internal and external fields, in *Lunar and Planetary Science XXXVII*, Abstract #1933, Lunar and Planetary Institute.

Richmond, N. C., L. L. Hood, D. L. Mitchell, R. P. Lin, M. H. Acuña, and A. B. Binder (2005), Correlations between magnetic anomalies and surface geology antipodal to lunar impact basin, *J. Geophys. Res.*, *110*, E05011, doi: 10.1029/2005JE002405.

Starukhina, L. V., and Y. G. Shkuratov (2004), Swirls on the moon and mercury: meteoroid swarm encounters as a formation mechanism, *Icarus*, *167*, 136–147.

Tsyganenko, N. A. (1996), Effects of the solar wind conditions on the global magnetospheric configuration as deduced from data-based field models, in *European Space Agency Publ. ESA SP-389*, pp. 181–185.

Wilhelms, D. E. (1987), *The geologic history of the Moon*, 256-258 pp., U.S. Geological Survey.